

The Effects of Silanation of External Acid Sites on the Structure and Catalytic Behavior of Mo/H–ZSM5

Weiping Ding,^{*,1} George D. Meitzner,[†] and Enrique Iglesia^{*,2}

^{*}Materials Sciences Division, E.O. Lawrence Berkeley National Laboratory and Department of Chemical Engineering, University of California at Berkeley, Berkeley, California 94720; and [†]Edge Analytical Inc., 2126 Allen Blvd #3, Middleton, Wisconsin 53562

Received April 3, 2001; revised October 15, 2001; accepted October 15, 2001; published online January 14, 2002

The selective silanation of external acid sites in H–ZSM5 using large organosilane reagents was used to decrease the density of such sites and the number of MoO_x species retained at external surfaces during cation exchange using MoO₃/H–ZSM5 physical mixtures. On samples prepared using silica-modified H–ZSM5, acid sites, MoO_x precursors, and the active MoC_x species formed during CH₄ reactions at 950 K reside predominately within zeolite channels, where spatial constraints inhibit bimolecular chain-growth pathways. As a result, these samples show higher selectivities to desired C₂–C₆ aromatics and lower deactivation rates than those prepared from untreated H–ZSM5. CH₄ conversion rates are also higher on Mo/H–ZSM5 samples prepared from silanated H–ZSM5, because of the more complete exchange and higher dispersion of MoO_x precursors. *In situ* X-ray absorption measurements showed that silanation of external OH groups does not influence the structure of the MoO_x precursors formed during synthesis or of active MoC_x species formed during CH₄ reactions from exchanged (Mo₂O₅)²⁺ dimers. The substantial absence of acidic OH groups and of MoC_x species sites at unconstrained external surfaces leads to significant improvements in activity, selectivity, and stability for Mo/H–ZSM5 catalysts for CH₄ pyrolysis reactions. © 2002 Elsevier Science (USA)

INTRODUCTION

The nonoxidative catalytic conversion of methane to aromatics on Mo/H–ZSM5 leads to high benzene selectivities at near-equilibrium CH₄ conversions (1–3). Recently, several other materials (e.g., Mo, W, Re, V, and Cr and their mixtures on H–ZSM5) have been reported to catalyze this reaction. Other zeolites, such as HZSM-11, HZSM-8, H-beta, HCMC-41, HY, and H–mordenite have also been used to disperse active metal, carbide, and oxide species (4–10). Mo/H–ZSM5 remains the most effective catalyst, but the near-equilibrium CH₄ conversions at which catalytic properties have been compared renders these conclusions

nonrigorous. Mo/H–ZSM5 catalysts deactivate to ~50% of their initial activity in ~10 h (11). Treatment by H₂ at reaction temperatures restores most of the initial activity, while treatment in air leads to the complete recovery of initial reaction rates (12). CH₄ and CO_x form during reactivation in H₂ and air, respectively, which suggests that deactivation arises from the formation of carbonaceous deposits (12).

Brønsted acid sites on external zeolite surfaces have been implicated in many unselective catalytic reactions. Such sites are easily accessed by reactants and are not protected against undesired side reactions by the shape-selective environment within zeolite channels (13–15). Coke and large hydrocarbons form at external surfaces because of the absence of spatial constraints; in contrast, steric restrictions within zeolite channels inhibit the formation of large activated complexes and hinder the formation of polynuclear aromatics and of alkylated benzenes larger than durene. In spite of the expected shape selectivity, Mo/H–ZSM5 catalysts form detectable amounts of naphthalene and larger aromatics from CH₄ (2, 16). The elimination of any external sites potentially responsible for these unselective pathways may inhibit the formation of deactivating carbon residues and increase the selectivity to benzene and to C₂–C₅ aliphatic hydrocarbons. This study addresses the synthesis and catalytic behavior of Mo/H–ZSM5 samples prepared via solid-state methods using H–ZSM5 materials, with their external acid sites titrated by the selective deposition of silica using large organosilane molecules that cannot enter ZSM5 channels. The results reported here show that silica deposition indeed increases hydrocarbon formation rates and decreases deactivation rates during CH₄ reactions on Mo/H–ZSM5 at high temperatures.

EXPERIMENTAL

Catalyst Synthesis and Silanation Methods

Silica-modified H–ZSM5. SiO₂/H–ZSM5 was prepared by immersing H–ZSM5 (Zeolyst International; Si/Al = 15;

¹ Permanent address: Department of Chemistry, Nanjing University, Nanjing 210093, China.

² To whom correspondence should be addressed. E-mail: iglesia@chem.berkeley.edu.

9.6 g) into an ethanol solution (100 cm³) containing 1.46 g of 3-aminopropyl-triethoxysilane (Aldrich, 99.9%) and subsequently evaporating the ethanol solvent at 333–393 K. The sample was then treated at 823 K for 16 h in dry air (1.67 cm³/s, 100 cm³/min) in order to decompose the organosilane precursors and to form the silica-modified H-ZSM5 (nominally 4% wt SiO₂/H-ZSM5). The strongly basic amino groups in 3-aminopropyl-triethoxysilane molecules lead to strong adsorption on acid sites, but the large size of the organosilane molecules prevent the titration of acidic OH groups within zeolite channels. Thus, only acid sites at the external surfaces react with these bulky silica precursors. After combustion of the organic component in anchored organosilane molecules, SiO_x species selectively replace external hydroxyls with SiO_x species lacking acidic hydroxyls (17, 18).

Solid-state exchange of MoO_x species onto ZSM5. SiO₂/H-ZSM5 was thoroughly mixed with the amount of MoO₃ (Johnson Matthey Electronics, 99.95%) required to prepare a sample with a nominal Mo content of 4% wt by grinding in an agate mortar for ~0.5 h, pressing into loose pellets, and crushing to granules (35–60 mesh). A sample with MoO_x species exchanged into SiO₂/H-ZSM5 was then obtained by treating these mixtures in air via procedures reported previously (11, 12) before characterization or catalytic measurements. This sample contains nominally 4% wt Mo and it is denoted as 4MoSi throughout. A similar procedure was used to prepare a sample using unmodified H-ZSM5 and denoted as 4Mo. Surface areas and micropore volumes (*t*-plot) before and after silica deposition were measured by N₂ adsorption at ~77 K (Quantachrome, Autosorb-6) (19).

Isothermal Reduction and Carburization Kinetics for 4Mo and 4MoSi Samples

The starting physical mixtures (4Mo or 4MoSi; 0.2 g) were heated in 20% O₂/He (Airgas, UHP; 1.67 cm³/s) at 10 K/min to 973 K and held for 0.5 h. This procedure leads to the quantitative exchange of MoO₃, predominantly as Mo oxo dimers (Mo₂O₅)²⁺ interacting with two exchange sites (11, 12). Samples were then cooled in He (1.67 cm³/s, Airgas, ultrahigh purity) to 950 K and the flow was changed to CH₄/Ar/He (1 : 1 : 3; 1.67 cm³/s, Airgas, ultrahigh). The concentrations of unreacted CH₄ and of reaction products were measured continuously by mass spectrometry (Leybold–Inficon Transpector 1.0). CH₄ conversion and product formation rates were obtained from these mass spectrometric data using Ar as an internal standard. The analysis of these complex product mixtures required frequent calibration of mass fragmentation patterns, as well as matrix deconvolution methods that account for common mass fragments formed from several types of molecules present in the product mixtures (20).

Isotopic Exchange of OH Groups Using D₂

The isotopic exchange of residual OH groups with D₂ was used to measure the density of OH groups remaining after silanation and MoO_x exchange (11, 12). The 4Mo and 4MoSi (0.2 g) samples were placed within a quartz tube and treated in 20% O₂/He (Airgas, UHP, 1.67 cm³/s) by increasing the temperature to 973 K at 10 K/min and holding for 0.5 h, using procedures reported previously for the exchange of MoO_x species (11, 12). After cooling to ambient temperature in He, a 5% D₂/Ar mixture (1 cm³/s; Matheson, UHP) was introduced and the sample temperature was increased to 973 K at 10 K/min and held at 973 K for 0.5 h. The amounts of HD and H₂ evolved during the exchange were measured by mass spectrometry (Leybold–Inficon, Transpector 1.0) using Ar as the internal standard.

Catalytic Methane Conversion on 4Mo and 4MoSi Samples

After *in situ* exchange within the reaction cell, samples (0.5 g) were flushed with He for 0.2 h at 973 K (0.67 cm³/s, UHP) in order to remove air from the cell. After cooling to 950 K, He was replaced with 50% CH₄/Ar (0.208 cm³/s (12.5 cm³/min), Praxair, UHP). The concentrations of unreacted CH₄, of the Ar inert, and of the products formed were measured by gas chromatography (Hewlett–Packard 5890). The concentrations of H₂, Ar, CH₄, CO, and CO₂ were measured using a Porapak Q column (3 mm × 2 m) and thermal conductivity detection. A methyl-silicone HP-1 capillary column (0.32 mm × 50 m) and a flame-ionization detector were used to measure CH₄, C₂H₄, C₂H₆, benzene, toluene, naphthalene, and traces of other hydrocarbons up to dimethyl-naphthalenes. CH₄ conversions were calculated using Ar as an internal standard. Selectivities are reported on a carbon basis, as the percentage of the CH₄ converted appearing as each detected reaction product. Products larger than dimethyl-naphthalenes form, but they do not reach the gas chromatograph through heated transfer lines maintained at 423 K. Therefore, the sum of selectivities is generally less than 100%. The products not detected are labeled as C₁₂₊ and calculated by difference.

X-Ray Absorption (XAS) Measurements

In situ XAS measurements (21, 22) were carried out using beamline 4-1 at the Stanford Synchrotron Radiation Laboratory. A two-crystal Si(220) monochromator was used and detuned by 30% in order to reject harmonics. The spectrum for a Mo foil was used to calibrate the energy scale by assigning the second inflection point to the Mo edge at 19.999 keV. The extended X-ray absorption fine structure (EXAFS) was analyzed using WinXas97 (23) (version 1.2) and FEFF7.0 (24). The code ATOMS (25) was used to generate initial atom positions from crystallographic data as a starting point in FEFF structural refinements. The *k*³-weighted EXAFS was Fourier-transformed in the range

0.3–1.5 nm⁻¹ and fitted in R-space to 0.8 nm. A Mo₂C cluster of radius 0.4 nm was used as the starting point in the structural refinement of the fine structure of carburized 4MoSi and 4Mo samples. Mo-neighbor interatomic distances (R), coordination numbers (CN), and energy shifts (ΔE_0) were refined using error-minimization techniques.

RESULTS AND DISCUSSION

Figure 1 shows HD evolution rates during D₂-OH exchange on the H-ZSM5 starting materials and on a SiO₂/H-ZSM5 sample after treatment in air at 973 K. Deactivation of external sites by silanation decreased the area and the temperature of the HD evolution peak, which suggests that the total number of OH groups decreases and that sites for the dissociation of D₂, the rate-controlling step in the exchange process (26), are introduced during silanation. Since the silica deposition procedures used were shown previously to titrate only external OH groups (17), we conclude that the observed decrease in OH density reflects the disappearance of external OH groups. The areas under the two curves in Fig. 1, which reflect the number of OH groups in each sample, indicate that ~24% of the OH groups in the starting material are removed by silanation (560 → 421 μmol/g). Silanation led also to a slight decrease in surface area (590 to 540 m²/g) and micropore volume (t -plot method, 0.12 to 0.106 cm³/g). This small decrease in surface area and micropore volume suggests that the silanation processes block a small fraction of the zeolite channels.

Figure 2 shows the effect of treatment temperature on the number of OH groups, measured from the combined

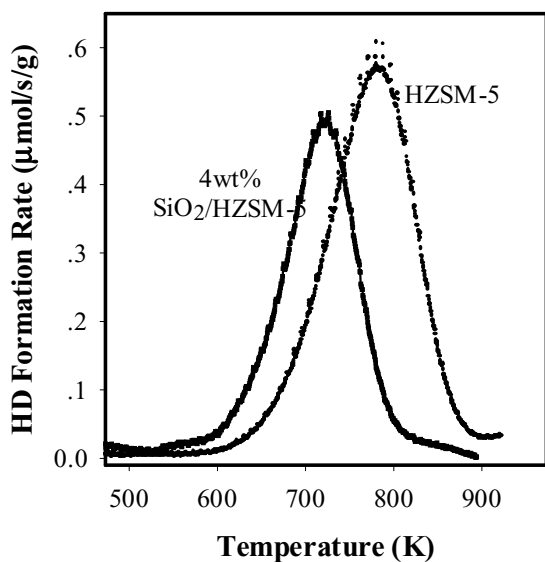


FIG. 1. Evolution of HD during D₂-OH exchange performed on H-ZSM5 before and after silica deposition (1 cm³/s 5% D₂/Ar, 10 K/min, 0.2 g of catalyst).

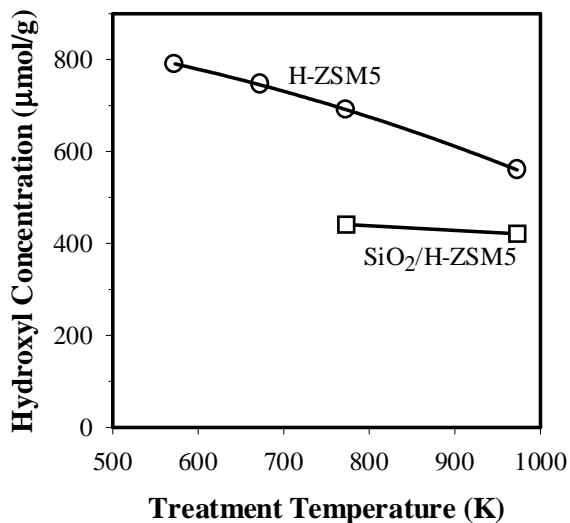
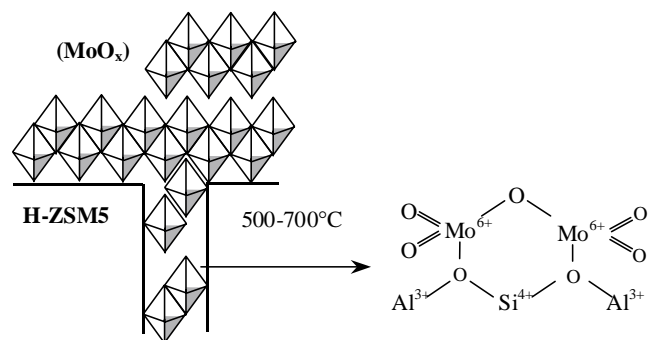


FIG. 2. Variation of OH groups of H-ZSM5 and SiO₂/H-ZSM5 with treatment temperature in 1.67 cm³/s 20% O₂/He.

amounts of HD and H₂ evolved during D₂-OH exchange, on H-ZSM5 and silica-modified H-ZSM5. The decline in hydroxyl density with increasing temperature reflects the removal of various types of OH species, including silanols, extraframework Al-OH, and vicinal acidic OH groups at Al framework sites via dehydroxylation reactions. The condensation of vicinal acidic OH groups leads to the distortion of tetrahedral framework Al atoms and to their ultimate nucleation as Al₂O₃ clusters at higher temperatures (27). The OH density was much less influenced by temperature on silica-modified H-ZSM5 than on unmodified H-ZSM5.

The exchange of MoO_x onto H-ZSM5 (Scheme 1) involves the initial spreading of a MoO₃ layer on ZSM5 external surfaces and the anchoring of these layers onto external OH groups (12). These layers then depolymerize at higher temperatures to form MoO_x monomers and small oligomers, which migrate into zeolite channels and react with OH groups to form (MoO₂OH)⁺ species. At even higher temperatures, (MoO₂OH)⁺ species react with



SCHEME 1. Molybdenum oxide species exchange into H-ZSM5 channels.

TABLE 1

Quantitative Results of OH Groups in Mo/H-ZSM5 Samples

Catalysts	Silica/		4Mo	4MoSi
	H-ZSM5	H-ZSM5		
OH density detected by HD exchange ($\mu\text{mol/g}$)	560 ^a	421 ^a	82	8.4
H in water evolved during heating in 673–973 K ($\mu\text{mol/g}$)	94	~10	562 ^b	424 ^b
Nominal Mo loading ($\mu\text{mol/g}$)	—	—	416	416
H removed per Mo ^c	—	—	1.15	0.99

^a Pretreated in 20% O₂/He before H–D exchange at 973 K.

^b From MoO₃/zeolite mixtures.

^c Calculated from HD exchange results.

either vicinal H⁺ in OH groups or with other (MoO₂OH)⁺ groups to evolve H₂O and to form anchored Mo monomers or dimers within zeolite channels. About one OH group is removed per Mo atom in the mixture (12), which suggests the predominant formation of (Mo₂O₅)⁺² dimers interacting with two exchange sites.

Table 1 shows the residual OH concentrations for H-ZSM5 and SiO₂/H-ZSM5 after treatment in dry air at 773 and 973 K. A larger number of OH groups (130 $\mu\text{mol/g}$) is removed between 773 and 973 K in H-ZSM5 than in SiO₂-H-ZSM5 (20 $\mu\text{mol/g}$); this is confirmed by the larger amount of H₂O evolved from H-ZSM5 during thermal treatment within this temperature range. Thus, it appears that the OH groups removed from H-ZSM5 during thermal treatment correspond to those titrated by silanation and residing predominately on external ZSM5 surfaces. These external OH groups can anchor MoO_x species during solid-state exchange and retain them in the unprotected environment of external surfaces, where they deactivate rapidly by overcarburization and carbon formation. Thus, it is likely that the ultimate location of exchanged MoO_x species may be strongly influenced by silanation of external OH groups before exchange. Also, acidic OH groups at external surfaces can catalyze uncontrolled oligomerization and aromatization reactions, leading to polynuclear aromatics that would not form within channels.

The introduction of MoO_x species into H-ZSM5 (4Mo) and SiO₂/H-ZSM5 (4MoSi) was monitored by measuring the amount of H₂O evolved during exchange. H₂O evolution occurs faster in 4MoSi than in 4Mo during heating in dry air (Fig. 3). The water evolution peak temperature decreased from 876 K on 4Mo to 857 K on 4MoSi. Also, a broad shoulder observed at ~970 K on 4Mo is not present in 4MoSi. These data suggest that MoO_x migration occurs slightly faster and more completely when H-ZSM5 is silanated before MoO_x exchange. This is likely to reflect the weaker anchoring of dissociated MoO₃ layers on silanated external surfaces, which lead to faster and more complete removal of the MoO_x species anchored on such external surfaces during thermal treatment. Specifically, the disappear-

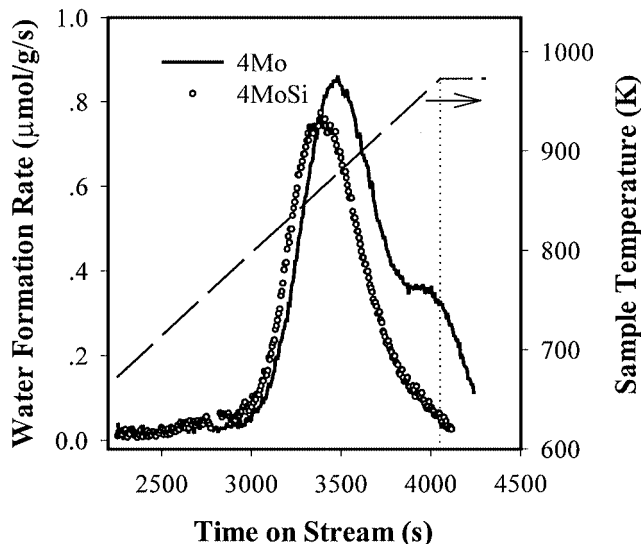


FIG. 3. Water evolutions during heating the physical mixture of MoO₃ with H-ZSM5 or silica-deposited H-ZSM5. (1.67 cm³/s 20% O₂/He, 10 K/min, 0.2 g of catalyst; water concentration was detected by mass spectrometry.)

ance of the broad high-temperature shoulder may reflect the substantial elimination of chemically bonded MoO_x at external sites by the removal of anchoring acidic hydroxyls by silanation before exchange.

D₂-OH isotopic exchange data from 4Mo and 4MoSi, after the MoO_x exchange process, but before CH₄ reaction, are shown in Fig. 4. The concentration of OH groups before and after introduction of Mo (from Figs. 1 and 4) and the amount of water removed during MoO_x exchange (from Fig. 3) are shown in Table 1. The exchange of MoO₃ onto H-ZSM5 during thermal treatment of physical

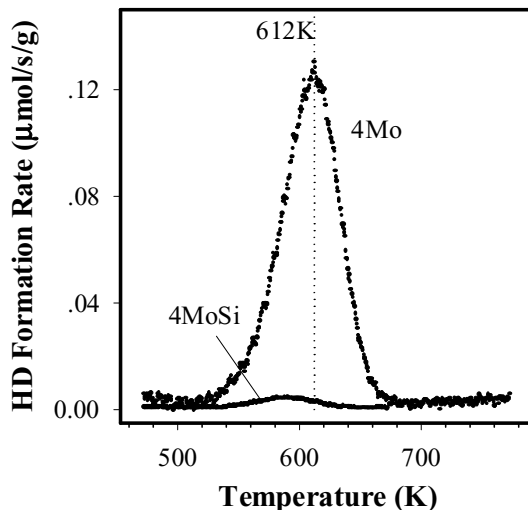


FIG. 4. HD evolution during D₂-OH exchange performed on 4Mo and 4MoSi after molybdenum solid exchange (1 cm³/s 5% D₂/Ar, 10 K/min, 0.2 g of catalyst).

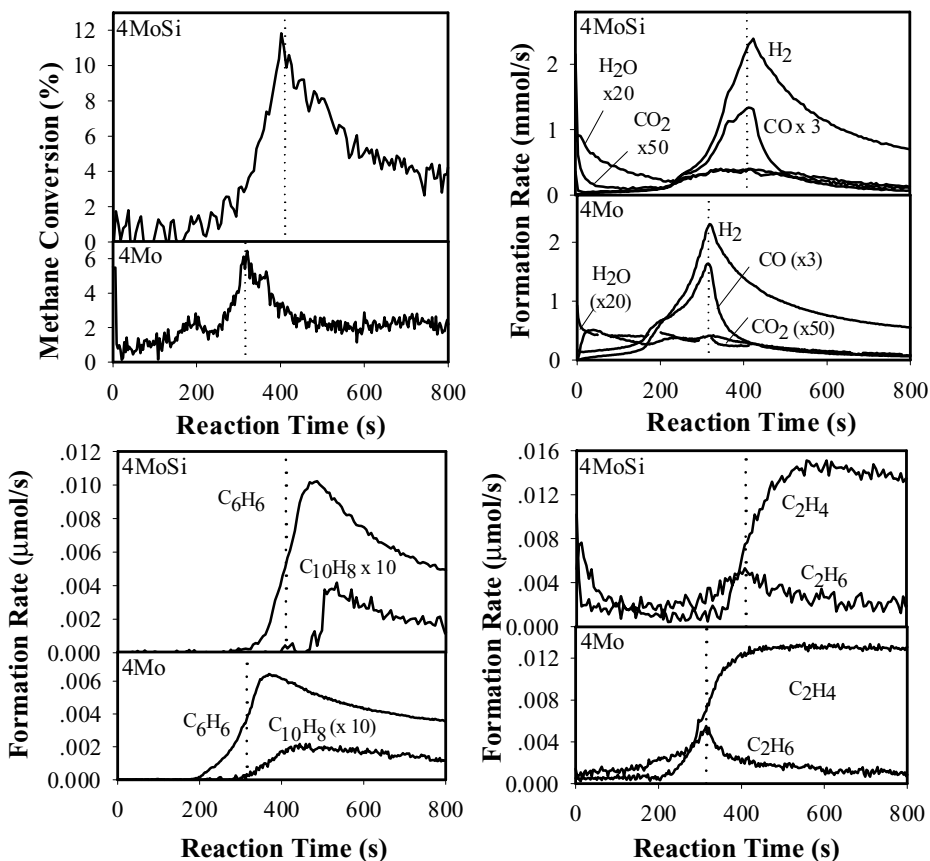


FIG. 5. Isothermal transient reaction of methane with 4Mo and 4MoSi. (950 K, $1.67 \text{ cm}^3/\text{s}$ $\text{CH}_4/\text{Ar}/\text{He}$ (1 : 1 : 3), ~ 1 bar, 0.2 g of catalyst, analysis by Leybold–Inficon Transceptor 1.0 quadrupole mass spectrometer.)

mixtures led to a decrease in the residual OH concentration from 560 to $82 \mu\text{mol/g}$ after exchange at 973 K. The number of OH groups removed per Mo was 1.15. In contrast, the OH concentration on 4MoSi decreased from 421 to $\sim 8 \mu\text{mol/g}$ after MoO_3 exchange (Table 1). The residual OH concentration was much lower than on 4Mo, and the number of removed OH groups per Mo was 0.99 in 4MoSi. This suggests that some OH groups are removed by OH condensation reactions, or that some MoO_x remove two OH groups on H–ZSM5, and that silica deposition eliminates such processes by removing external OH groups.

Table 1 also shows the number of H-atoms removed as water from H–ZSM5 during treatment in O_2/He from 673 to 973 K. Silanation significantly decreased the amount of water evolved from H–ZSM5 at these temperatures. We infer from these data that the larger amount of water removed from H–ZSM5 arises from external OH groups, which can bind MoO_x species during the initial stages of exchange and release them for migration and exchange at higher temperatures (water evolution shoulder in Fig. 3). Silanation removed such binding sites before thermal treatment of $\text{MoO}_3/\text{H-ZSM5}$ physical mixtures. The selective removal

of external OH groups improves the efficiency and completeness of the MoO_x exchange onto intrachannel sites.

Figure 5 shows the rate of CH_4 conversion and of hydrocarbon formation at 950 K on 4Mo and 4MoSi samples prepared by thermal treatment of physical mixtures within the catalytic reactor during initial contact with CH_4 . Both samples showed initial induction periods (~ 150 s for 4Mo and ~ 300 s for 4MoSi), during which CH_4 conversion was very low. After this initial period, CH_4 conversion rates increased sharply, with the predominant formation of CO_x , H_2 , and H_2O , and then decreased with increasing reaction time, as the products became exclusively hydrocarbons and H_2 . The induction period reflects the autocatalytic nature of the reduction of Mo(VI) species, which catalyze C–H bond activation in CH_4 with increasing efficiency as more sites are generated by reduction and carburization of the exchanged MoO_x species. The details of these initial reduction and carburization process have been previously described (28). Here, we note only that silanation delays the onset of reduction and of CH_4 conversion; silica also eliminates a small CH_4 consumption peak at ~ 200 s, observed on the 4Mo sample before the main CH_4 peak (Fig. 5). This peak

reflects the presence of easily reduced MoO_x species present at low concentrations on the unmodified H-ZSM5. These species reduce and carburize at lower temperatures than do the exchanged $(\text{Mo}_2\text{O}_5)^{2+}$ dimers and do not form on the H-ZSM5 precursors modified by silanation of their external surfaces. Thus, it appears that MoO_x domains at external surfaces form by interactions with hydroxyls available on the external surfaces of unmodified H-ZSM5; these MoO_x clusters are more accessible and probably also larger in size than the prevalent $(\text{Mo}_2\text{O}_5)^{2+}$ dimers located at exchange sites located within ZSM5 channels. The reduction and carburization of these external MoO_x species in 4Mo samples then leads to sites capable of activating CH_4 and of generating H_2 . In turn, the H_2 formed can be used to initiate the reduction of exchanged MoO_x dimers, and it shortens the induction period required for the reduction and carburization of exchanged dimers. MoO_x exchange from physical mixtures containing silanated H-ZSM5 (4MoSi) consequently shows longer induction periods, because they lack external MoO_x species that catalyze CH_4 activation and the formation of H_2 at lower temperatures than exchanged MoO_x species.

During the induction period, MoO_x species reduce to lower valent Mo species. This process is followed by carburization, during which C and H atoms from CH_4 molecules are used to form the CO_x , H_2O , and H_2 observed during the initial stages of CH_4 reactions. The resulting MoC_x species provide the active sites for rate-determining C-H bond activation steps. The reduction-carburization of exchanged MoO_x species also reforms the internal acidic OH groups removed during Mo exchange and required for acid-catalyzed oligomerization and aromatization reactions of the light alkenes initially formed from CH_4 (16, 29). The reduction and carburization of MoO_x appears to be complete in ~ 800 s on both 4Mo and 4MoSi samples (Fig. 5).

Steady-state catalytic data are shown in Figs. 6 and 7 for 4Mo and 4MoSi samples. The rate of CH_4 conversion decreased gradually with time on stream on both 4Mo and 4MoSi, but they are always higher on 4MoSi than on 4Mo at all contact times (e.g., 1.6 mol/g-atom Mo-s vs 1.2 mol/g-atom Mo-s on 4Mo at 5 h onstream). For a given CH_4 conversion level, 4MoSi gives a higher selectivity to benzene and a lower selectivity to naphthalene and to C_{12+} hydrocarbons than does 4Mo. The higher CH_4 conversion rates achieved on the Si-modified sample reflect the more complete exchange of Mo species during synthesis and the consequently higher density of MoC_x sites accessible for rate-determining steps. The lower selectivity to higher molecular weight aromatics suggests that reactions occur more frequently within constrained channels when hydroxyl groups on external surfaces have been removed by silanation and they are no longer available to anchor MoO_x precursors and MoC_x active species. As a result, a larger fraction of C-H bond activation steps and of the acid-catalyzed

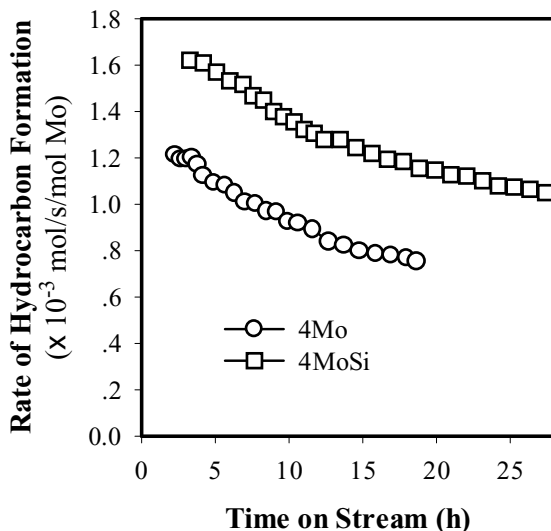


FIG. 6. Hydrocarbon formation rate (mol/mol Mo-s) as a function of contact time on 4Mo and 4MoSi (950 K, 12.5 cm³/min CH₄/Ar (1:1), 0.5 g of catalyst, ~ 1.1 bar).

oligomerization and aromatization reactions that follow these steps occurs within zeolite channels that restrict chain growth.

Naphthalene selectivities are slightly lower on 4MoSi than on 4Mo (~ 13 vs $\sim 11\%$ at 7% CH_4 conversion) and C_{12+} selectivities are much lower (~ 19 vs 11%). It appears that naphthalene forms both within and outside zeolite channels, but at higher rates on unconstrained external sites removed by the silanation procedure. C_{12+} products contain polynuclear aromatics that form preferentially outside zeolite channels, but also coke that forms within zeolite channels and in homogeneous reactions at these reaction temperatures. These results demonstrate that significant improvements in the selectivity to benzene on Mo/H-ZSM5 can be achieved by the selective elimination of acid sites and of MoO_x species from external zeolite surfaces. Zeolite channels in H-ZSM5 effectively restrict the chain-growth pathways required to form naphthalene and methylnaphthalenes, even at ~ 1000 K, apparently by inhibiting the molecular collisions required to form polynuclear aromatics.

Figure 8 shows a semilogarithmic plot of the hydrocarbon formation rate as a function of time on stream on 4Mo and 4MoSi. First-order deactivation rate constants are significantly smaller on 4MoSi (0.018 h^{-1}) than on 4Mo (0.030 h^{-1}). The higher average molecular weight of the products made on 4Mo (Fig. 7) also suggests a higher tendency to form H-deficient large hydrocarbons, which are likely intermediates in the formation of deactivating residues.

Previously, we showed that the $(\text{Mo}_2\text{O}_5)^{2+}$ dimers interacting with Al sites form during exchange by replacing

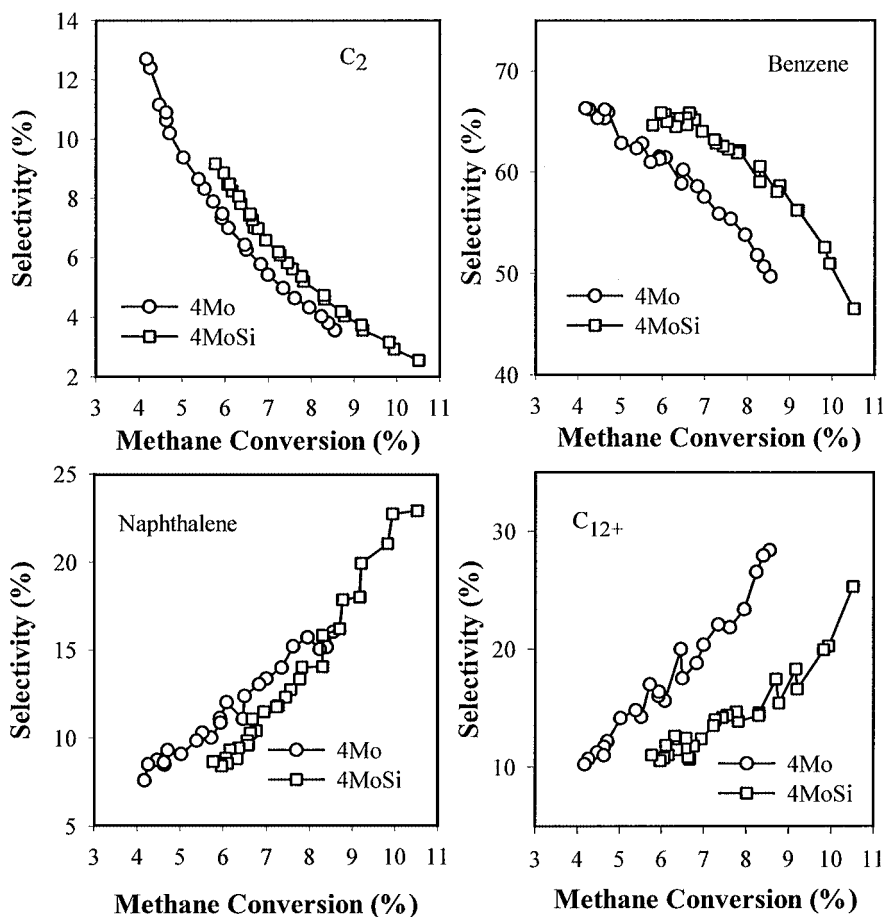


FIG. 7. Selectivity to various hydrocarbons as a function of CH_4 conversion on 4Mo and 4MoSi (950 K, $12.5 \text{ cm}^3/\text{min}$ CH_4/Ar (1:1), 0.5 g of catalyst, ~ 1.1 bar).

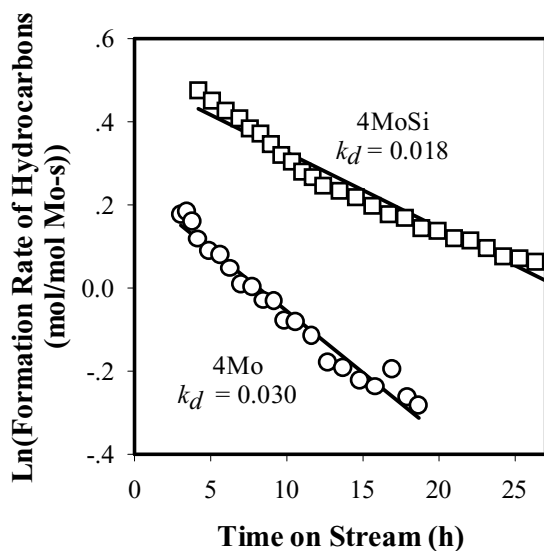


FIG. 8. Methane conversion rate as a function of contact time on 4Mo and 4MoSi. (k_d is calculated from slope of semilogarithmic plot (950 K, $12.5 \text{ cm}^3/\text{min}$ CH_4/Ar (1:1), 0.5 g of catalyst, ~ 1.1 bar).

two acidic OH groups, but such OH groups are regenerated during reduction and carburization of these dimers to form MoC_x clusters during CH_4 reactions at ~ 950 K (29). Most of the acidic OH sites initially replaced by Mo oxo species during exchange are restored and the two sites required for CH_4 conversion, MoC_x and acidic hydroxyls, form *in situ* from the $\text{Mo}_2\text{O}_5^{2+}$ dimer and the CH_4 reactants. Figure 9 shows Mo K-edge XAS spectra collected at ambient temperature for 4MoSi, 4Mo, and a bulk Mo_2C synthesized *in situ* by carburization of bulk MoO_3 (30); the first two of these samples were used for reactions of CH_4 at 950 K before collecting the XAS spectra without intervening exposure to ambient air between the reaction and the collection of the spectra. On both catalysts, the Mo–K absorption edge shifts to lower energies during CH_4 reactions at 950 K ($\Delta E_0 \sim 5$ eV), and a preedge feature corresponding to an electronic transition into a bound state in Mo(VI) disappears, consistent with the reduction of Mo(VI) centers.

The k^3 -weighted experimental and simulated molybdenum radial distribution functions are shown in Fig. 10 after

TABLE 2

MoC_x Structures in 4Mo and 4MoSi during Methane Reaction

Catalyst	Mo–C Shell			Mo–Mo Shell		
	CN	Distance/Å	$\sigma^2/\text{Å}^2$	CN	Distance/Å	$\sigma^2/\text{Å}^2$
4Mo ^b	1.1 ± 0.20	2.074 ± 0.021	0	3.4 ± 0.8	2.971 ± 0.011	0.005 ± 0.002
4MoSi ^c	2.3 ± 0.29	2.081 ± 0.013	0	3.2 ± 0.7	2.968 ± 0.020	0.006 ± 0.003

^a σ^2 : Debye–Waller factor; it was fixed to zero in fitting for Mo–C shell.

^b Spectra were collected on 4Mo after *in situ* 6.33-h methane reaction.

^c Spectra were collected on 4MoSi sample after 25-h *ex situ* and 1-h *in situ* methane reaction.

in situ CH₄ reaction at 950 K. The structural parameters for the Mo–C species formed, obtained by fitting the Mo–K extended X-ray absorption fine structure (EXAFS), are shown in Table 2. The details of the analysis method have been described previously (29). The Mo–Mo coordination number (CN) for 4MoSi was ~3.2 after reaction for 26 h, and 3.4 for 4Mo after 6.3 h CH₄ reaction. The values of about 3 for the Mo–Mo first-shell coordination are consistent with the ~0.6-nm Mo₂C cluster shown in the inset of Fig. 10 (31). These results indicate that both 4Mo and 4MoSi consist of small MoC_x clusters during CH₄ reaction at 950 K. Silanation does not influence the structure of the majority MoC_x species, the size of which is consistent with their predominant location within zeolite channels.

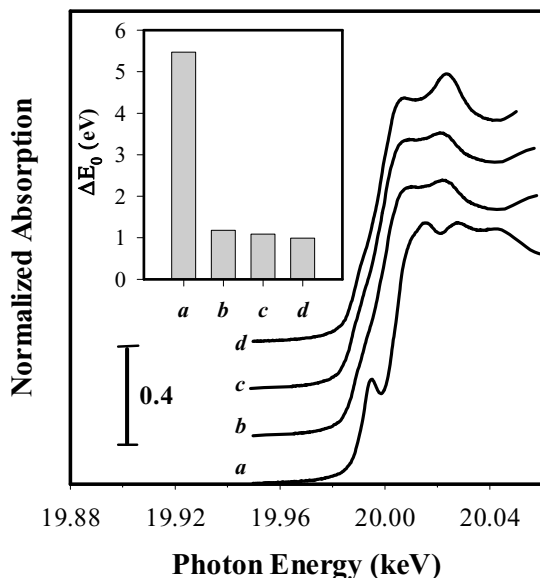


FIG. 9. Mo–K X-ray absorption near-edge spectra collected *in situ* at room temperature on 4Mo and 4MoSi. Inset shows Mo–K edge energies referenced to Mo foil. (a) Physical mixture of MoO₃ with H–ZSM5; (b) 4Mo after *in situ* 6.33-h methane reaction (955 K, 24 mg of catalyst, 1 cm³/min CH₄/Ar (1/1)); (c) 4MoSi after 25-h *ex situ* (950 K, 0.5 g of catalyst, 12.5 cm³/min CH₄/Ar (1/1)) and 1-h *in situ* methane reaction (955 K, ~20 mg of catalyst, 1 cm³/min CH₄/Ar (1/1)); (d) *in situ* synthesized bulk Mo₂C (Ref. 29a).

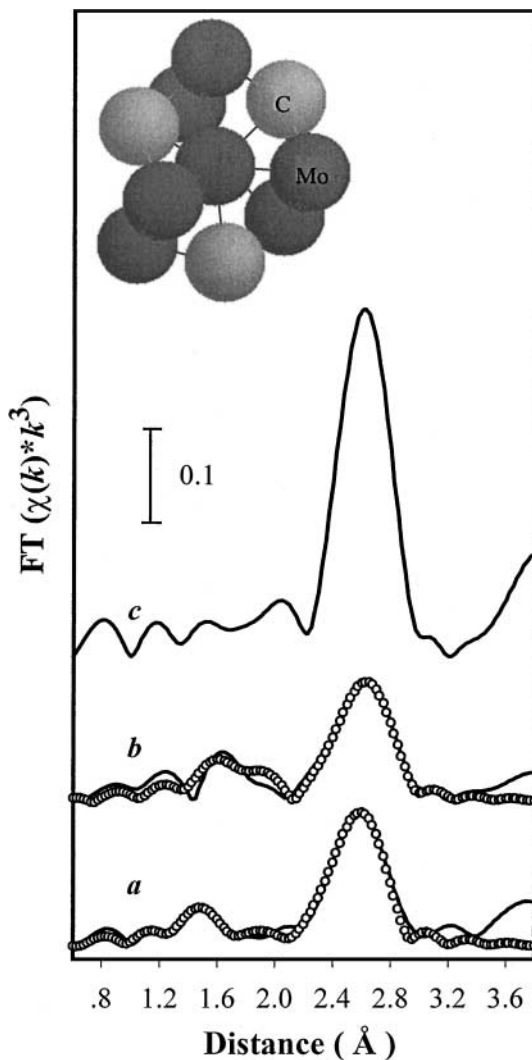


FIG. 10. Mo radial distribution functions. (a) 4Mo after *in situ* 6.33-h methane reaction; (b) 4MoSi after 25-h *ex situ* and 1-h *in situ* methane reaction; (c) *in situ* synthesized bulk Mo₂C. Lines, Experimental data; dots, fitted data. (Inset shows Mo–C cluster with Mo₂C crystal structure and diameter of about 0.6 nm, derived from Ref. 30. Conditions for sample treatment are the same with those for Fig. 9.)

CONCLUSIONS

Silanation decreases the density of acid sites on external H-ZSM5 surfaces and the number of MoO_x species deposited at such external surfaces during exchange from physical mixtures of MoO₃ and H-ZSM5. In this way, acidic OH groups, MoO_x precursors, and the active MoC_x species formed during CH₄ reaction are preferentially located within zeolite channels, where spatial constraints inhibit the bimolecular events and transition states are required for the formation of large polynuclear aromatics. Mo/H-ZSM5 catalysts prepared by exchange of silanated H-ZSM5 lead to higher reaction rates, because of more complete exchange of MoO_x precursors, to higher selectivities to one-ring aromatics, and to slower deactivation, because reactions occur preferentially within shape-selective environments. The silanation of external OH groups does not influence the structure of the active MoC_x species formed during CH₄ reactions.

ACKNOWLEDGMENTS

We acknowledge financial support from the Division of Fossil Energy of the U.S. Department of Energy (Contract DE-AC03-76SF00098) and the technical guidance of Dr. Daniel Driscoll. X-ray absorption data were collected at the Stanford Synchrotron Radiation Laboratory (SSRL), operated by the Office of Energy Sciences of the U.S. Department of Energy (DOE) under contract DE-ACO3-76SF00515. One of the authors (WD) acknowledges a leave of absence granted by Nanjing University in order to perform these studies at the University of California at Berkeley.

REFERENCES

- Guczi, L., van Santen, R. A., and Sarma, K. V., *Catal. Rev.* **38**, 249 (1996).
- Xu, Y. D., and Lin, L. W., *Appl. Catal. A* **188**, 53 (1999).
- Wang, L. S., Tao, L. X., Xie, M. S., Xu, G. F., Huang, J. S., and Xu, Y. D., *Catal. Lett.* **21**, 35 (1993).
- (a) Weckhuysen, B. M., Wang, D. J., Rosynek, M. P., and Lunsford, J. H., *J. Catal.* **175**, 338 (1998); (b) Weckhuysen, B. M., Wang, D. J., Rosynek, M. P., and Lunsford, J. H., *J. Catal.* **175** (2), 347 (1998).
- Zhang, C. L., Li, S., Yuan, Y., Zhang, W., Wu, T., and Lin, L. W., *Catal. Lett.* **56**, 207 (1998).
- Liu, S. T., Wang, L. S., Ohnishi, R., and Ichikawa, M., *J. Catal.* **181**, 175 (1999).
- Shu, Y. Y., Ma, D., Bao, X. H., and Xu, Y. D., *Catal. Lett.* **66** (3), 161 (2000).
- Xu, Y. D., Liu, S. T., Wang, L. S., Xie, M. S., and Guo, X. X., *Catal. Lett.* **30**, 135 (1995).
- Shu, Y. Y., Xu, Y. D., Wong, S. T., Wang, L. S., and Guo, X. X., *J. Catal.* **170**, 11 (1997).
- (a) Xu, N., Kan, Q. B., Li, X. M., Liu, Q. S., and Wu, T. H., *Chem. J. Chinese U.* **21** (6), 949 (2000); (b) Xu, N., Kan, Q. B., Zhang, J., Li, X. M., Ji, L., and Wu, T. H., *Chem. J. Chinese U.* **21** (7), 1113 (2000).
- Borry, R. W., Lu, E. C., Kim, Y. H., and Iglesia, E., *Stud. Surf. Sci. Catal.* **119**, 403 (1998).
- Borry, R. W., Kim, Y. H., Huffsmith, A., Reimer, J. A., and Iglesia, E., *J. Phys. Chem. B* **103**, 5787 (1999).
- Bhat, Y. S., Das, J., Rao, K. V., and Halgeri, A. B., *J. Catal.* **159**, 368 (1996).
- Melson, S., and Schuth, F., *J. Catal.* **170**, 46 (1997).
- Kunieda, T., Kim, J. H., and Niwa, M., *J. Catal.* **188**, 431 (1999).
- Kim, Y. H., Borry, R. W., and Iglesia, E., *Micropor. Mesopor. Mat.* **35**, 495 (2000).
- Our previous work showed that the ratio of Si/Al of H-ZSM5 analyzed by XPS increased linearly with the amount of silica (<4%) deposited using 3-aminopropyl-triethoxysilane as precursor, indicating that the silica was mainly deposited on the external surface of H-ZSM5. Meanwhile, XRD measurements revealed the same structure and crystallinity of silica deposited on H-ZSM5 as was found with the original H-ZSM5; results of adsorption measurements showed little change in isothermal adsorption of benzene and in the starting adsorption rate of *n*-hexane on silica deposition. Results of 4-methylquinoline adsorption revealed that most of the external surface acid sites were titrated by silica deposition. These results led to the conclusion that silica deposition with the method described in this report deactivated only the external surface of H-ZSM5.
- Loos, J. B., *Zeolites* **18**, 278 (1997).
- Gregg, S. J., and Sing, K. S. W., "Adsorption, Surface Area and Porosity." Academic Press, San Diego, 1982.
- Price, G. L., and Iglesia, E., *Ind. Eng. Chem. Res.* **28** (6), 839 (1989).
- Meitzner, G., and Iglesia, E., *Catal. Today* **53**, 433 (1999).
- Barton, D. G., Soled, S. L., Meitzner, G. D., Fuentes, G. A., and Iglesia, E., *J. Catal.* **181**, 57 (1999).
- WinXAS97 is an XAS data analysis program, for PCs running MS-Windows, by Thorsten Ressler (E-mail: t_ressler@compuserve.com; webpage: http://ourworld.compuserve.com/homepages/t_ressler).
- Rehr, J. J., Albers, R. C., and Zabinsky, S. I., *Phys. Rev. Lett.* **69**, 3397 (1992).
- The code ATOMS was written by Bruce Ravel (E-mail: ravel@u.washington.edu) to calculate coordination numbers and interatomic distances from compounds with known structures, and all input for FEFF7.0.
- Biscardi, J. A., Meitzner, G. D., and Iglesia, E., *J. Catal.* **179**, 192 (1998).
- Deng, F., Yue, Y., and Ye, C. H., *J. Phys. Chem. B* **102**, 5252 (1998).
- Arnold, P., de Jonge, J. C. M., and Moulijn, J. A., *J. Phys. Chem.* **89**, 4517 (1985).
- (a) Ding, W. P., Li, S., Meitzner, G. D., and Iglesia, E., *J. Phys. Chem. B* **105**, 506 (2001); (b) Li, W., Meitzner, G. D., Borry, R. W., and Iglesia, E., *J. Catal.* **191**, 373 (2000).
- Oyama, S. T., *Catal. Today* **15** (2), 179 (1992).
- Epiciet, T., Dubois, J., Esnouf, C., Fantozzi, G., and Convert, P., *Acta Metall.* **36**, 1903 (1998).